

Geometry of the (2×1) reconstruction of diamond (111)

This article has been downloaded from IOPscience. Please scroll down to see the full text article.

2002 J. Phys.: Condens. Matter 14 3085

(<http://iopscience.iop.org/0953-8984/14/12/301>)

View [the table of contents for this issue](#), or go to the [journal homepage](#) for more

Download details:

IP Address: 171.66.16.27

The article was downloaded on 17/05/2010 at 06:21

Please note that [terms and conditions apply](#).

Geometry of the (2×1) reconstruction of diamond (111)

S Walter¹, J Bernhardt¹, U Starke¹, K Heinz¹, F Maier², J Ristein² and L Ley²

¹ Lehrstuhl für Festkörperphysik, Universität Erlangen-Nürnberg, Staudtstrasse 7, D-91058 Erlangen, Germany

² Institut für Technische Physik II, Universität Erlangen-Nürnberg, Staudtstrasse 7, D-91058 Erlangen, Germany

E-mail: kheinz@fkp.physik.uni-erlangen.de

Received 31 January 2002

Published 15 March 2002

Online at stacks.iop.org/JPhysCM/14/3085

Abstract

A quantitative analysis of the (2×1) reconstruction of the diamond (111) surface by low-energy electron diffraction (LEED) is presented. Spot intensity versus energy data, $I(E)$, were collected for normal incidence up to electron energies of 500 eV and analysed using the tensor LEED perturbation method. A close fit between experimental and calculated data (according to a Pendry R -factor $R = 0.19$) confirms the model of π -bonded chains at the very surface, wherein neighbouring chains are at different heights equivalent to a considerable surface corrugation (0.68 Å). We find that the chains are practically untilted, i.e. the buckling within the chains is negligible (≤ 0.01 Å). The possible dimerization of the chains is also very small (relative bond-length difference $d = 0.7\%$), though the respective limits of error would allow values up to about 7%. For the subsurface structure we find that the surface reconstruction extends rather deep into the surface according to the considerable buckling amplitudes within sublayers down to the fourth bilayer. All structural parameters retrieved, including the negligible tilt and dimerization of chains as well as the extension of the surface reconstruction to deeper layers, are in excellent quantitative agreement with the results of *ab initio* calculations, so controversies existing up to now in the literature appear to be resolved.

1. Introduction

As diamond is a promising candidate for future semiconductor applications and as the sizes of devices are becoming ever smaller, the knowledge and understanding of its surface properties are important. This applies in particular to the (111) surface, which is the natural cleavage plane (with one bond per atom cut) but reconstructs after annealing to above 900 °C.

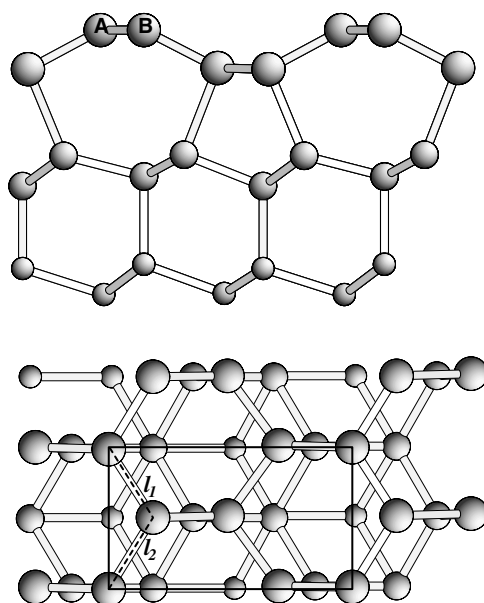


Figure 1. Pandey's π -bonded chain model for C(111) (2×1) in side view (top panel, projection on $(10\bar{1})$) and top view with the (2×1) unit cell indicated (bottom panel).

The reconstruction corresponds to a (2×1) superstructure as is evident from low-energy electron diffraction (LEED) when slightly miscut samples are used. In this case, the three equivalent 120° rotational domains are of different weight and the degeneracy of beams leading to an apparent (2×2) periodicity is lifted [1]. For the atomic arrangement accounting for the reconstruction, a chain-like structure dominated by π -bonding has been proposed by Pandey [2], similar to that proposed [3] and confirmed for the (2×1)-reconstructed (111) surfaces of Si [4–7] and Ge [7, 8]. As schematically displayed in figure 1, the truncation of surface bonds leads to an atomic reordering from which chains in $[10\bar{1}]$ direction result (see the bottom panel) and fivefold and sevenfold rings are formed by the atoms of the first and second bilayer (see the upper panel).

This π -bonded chain model has been confirmed in many investigations, including a quantitative LEED study [9] in which, however, only a few parameters could be determined. Generally, the precise structure of the unit cell is at best unclear, if not controversial. The degrees of freedom within that model preserving the (2×1) unit cell are

- *tilted* chains, with atoms A and B (see figure 1) at different heights so that there is an intrachain buckling and/or
- intrachain *dimerization*, i.e. alternating bond lengths within a chain ($l_1 \neq l_2$; see figure 1).

Certainly, there can be a combination of the two modifications. Such an asymmetry in the chains is required by the observation of a gap in the electronic band structure along the JK direction of the surface Brillouin zone (i.e. in the direction perpendicular to the chains) using angle-resolved photoemission spectroscopy [10, 11] or electron energy-loss spectroscopy [12, 13]. Whilst tilted chains are confirmed both experimentally and theoretically for Si and Ge (see [7] and references therein), the situation is rather unclear for diamond. By means of x-ray diffraction [14], a considerable tilt (buckling amplitude 0.30 \AA) of the same order of magnitude as for Ge and Si was deduced and found consistent with ion scattering measurements [15].

The interpretation of infrared–visible sum-frequency-generation spectroscopy data [16] also requires a (small) buckling of chains. Yet, with only two exceptions [17, 18], theoretical investigations (in particular *ab initio* calculations) predict untilted and undimerized chains within the limits of numerical accuracy [2, 7, 19–24].

To resolve this apparent misfit between theory and experiment we present a detailed quantitative LEED study of C(111) (2×1) . This method was chosen as it is very sensitive to vertical parameters with error limits in the pm range frequently reported [25, 26]. This precision is in particular possible when, as in the present case, normal-incidence data are used and a large database is available. So, the method should resolve tilted, i.e. vertically buckled, chains if present. On the other hand, normal-incidence LEED is less sensitive to lateral parameters (because of the comparably small lateral momentum transfer in the electron scattering process), so we cannot expect to safely detect a possible dimerization if it is small. Nevertheless, the estimation of an upper limit of dimerization should be possible. Additionally, we aim to determine the strength and depth of multilayer relaxation which is especially important in view to the subsurface stress caused by the (2×1) reconstruction, but experimentally unresolved as yet. All results will be compared to those of theoretical work, so illuminating our present understanding of the C(111) (2×1) reconstruction.

2. Experimental and computational details

2.1. Experiment

The crystal under investigation was a natural type-IIb (i.e. boron-doped) single crystal with a polished (111) surface. To start with a well defined initial state for preparation, the sample was subjected to an *ex situ* dry chemical process: a 15 min exposure to a microwave hydrogen plasma at 800 °C. Introduced in the UHV chamber, the sample immediately exhibited a sharp (1×1) LEED pattern indicative of a bulk-like-terminated but hydrogen-covered surface. Additional annealing at about 1200 °C produced a clear (2×1) diffraction pattern. By evaluation of the intensities of nominally symmetrically equivalent fractional-order beams it could be shown that the pattern is due to three rotational domains with a weight ratio of 56:26:18.

For the LEED intensity measurements a computer-controlled video-based measurement technique was applied allowing for fast data acquisition at a low primary-electron beam current [25]. With the low current, charging of the sample is avoided when the measurement is with the sample at room temperature, so providing sufficient electrical conductivity. Thermal diffuse scattering at this temperature is still small due to the high Debye temperature of diamond (2230 K), so spot intensities are only little reduced and high-quality intensity measurements are possible. The normal incidence of the primary-electron beam was adjusted by comparing the spectra of nominally equivalent beams, where the Pendry *R*-factor *R* was used as a quantitative measure [27]. For the eventual data set, the influence of residual misalignment was further reduced by final averaging of equivalent spectra. Five integer-order and seven fractional-order beams constitute a database of energy width $\Delta E = 3500$ eV.

2.2. LEED intensity analysis

The intensity analysis was performed by application of the tensor LEED (TLEED) perturbation scheme using the TensErLEED program package [28]. Atomic phase shifts were included up to an angular momentum of $l_{max} = 7$. Bilayers were treated as composite layers and then stacked by use of the layer-doubling scheme [29]. The inelastic electron attenuation was described by an imaginary potential, $V_{0i} = -7.0$ eV. For the structural search and optimization, a fast

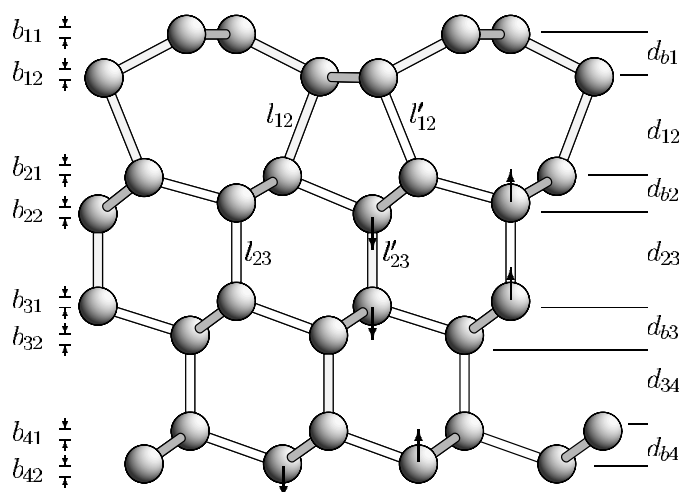


Figure 2. A side view of the π -bonded chain model exhibiting the main structural parameters determined (the optimized parameter values are given in table 1). The quantity b_{ij} denotes the buckling amplitude within the j th subplane of the i th bilayer, and the arrows give the directions of the main shifts of the atoms. Similarly, d_{bi} gives the intrabilayer buckling, i.e. the spacing between the centre-of-mass planes of the upper and lower subplanes within the bilayer i . The quantity d_{ij} denotes the spacing between the centre-of-mass planes of neighbouring bilayers i and j , whilst l_{ij} and l'_{ij} stand for the two symmetry-inequivalent bond lengths between the i th and j th layers.

search algorithm based on a frustrated simulated annealing procedure was applied [30], as also provided by the program package used. The search was guided and the agreement between calculated and experimental spectra quantified using again the Pendry reliability factor R [27]. The real part of the inner potential was continuously refined during each set of TLEED calculations.

To optimize the agreement between experimental and calculated spectra, the three coordinates of all atoms in the first and second bilayers and the vertical coordinates of all atoms in the third and fourth bilayers were varied. This amounts to a total of 32 structural parameters. The related interlayer spacings, buckling amplitudes and bond lengths are depicted in figure 2. Further, the vibrational amplitudes of the first two atomic layers were varied, whilst the vibrational amplitudes of deeper-layer atoms were kept fixed according to the bulk Debye temperature of diamond (2230 K). The error limits for a given parameter were estimated by its variation and the corresponding variation of the R -factor. Only parameter values leading to R -factors larger than $R_{min} + \text{var}(R_{min})$ (with $\text{var}(R_{min}) = R_{min}\sqrt{8V_{0i}/\Delta E}$ [27]) are supposed to be beyond the limits of errors. We emphasize that by this procedure, during which all other parameters are kept fixed at their best-fit values, correlations between different parameters are neglected.

3. Results

The structural search leads to a best fit between experimental and calculated model spectra according to $R_{min} = 0.19$ ($\text{var}(R_{min}) = 0.02$). The corresponding visual comparison of the spectra as displayed in figure 3 appears equally favourable, with practically all spectral features well reproduced. Error limits as estimated by $\text{var}(R_{min})$ amount to 0.03 Å for the vertical atomic coordinates in the first two bilayers, whilst the error for lateral parameters is 0.10 Å. For atomic positions in deeper layers, the errors increase because of the reduced sensitivity due to electron attenuation.

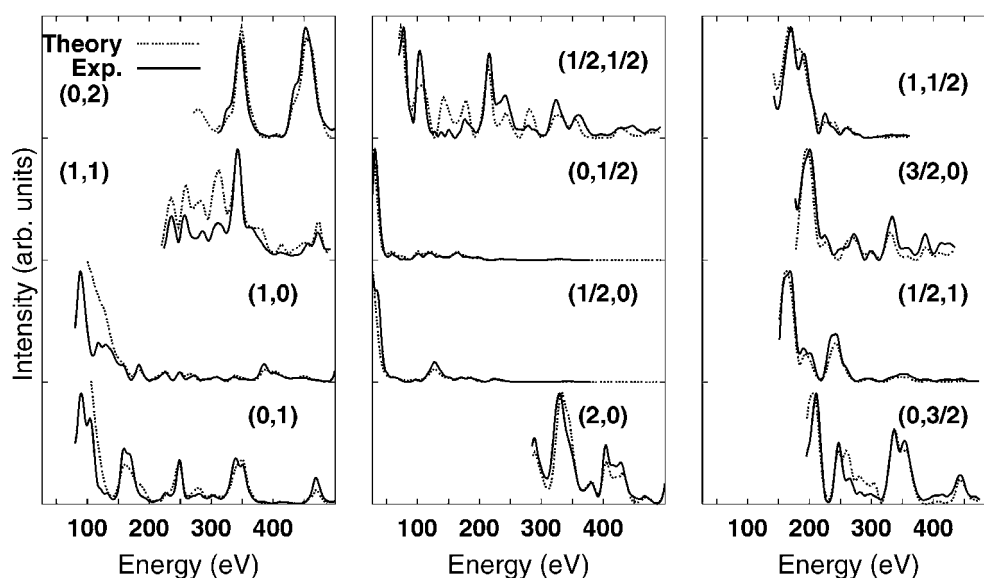


Figure 3. Comparison of experimental (solid curves) and best-fit calculated (dotted curves) $I(E)$ spectra.

First of all, the good agreement between experimental and computed spectra confirms once more the π -bonded chain model for C(111) (2×1) . The question of whether the chains are tilted or not is answered by table 1 which summarizes the vertical parameters determined in terms of interlayer spacings, buckling amplitudes and subsurface bond lengths as defined in figure 2. As is obvious, there is no, or at most an extremely small tilt of the chains, as the best-fit values of the corresponding buckling amplitudes b_{11} and b_{12} amount to only 0.01 Å, even smaller than the error limit of 0.04 Å estimated for the difference of the vertical coordinates. This result is clearly at variance with the above-mentioned x-ray structure determination [14] reporting an amplitude as large as 0.30 Å. This latter value is well outside our limits of errors because, as tested, it produces an R -factor of $R = 0.40$ whilst our error level amounts to $R_{min} + var(R_{min}) = 0.21$. We have no explanation for this disagreement, but remind the reader that x-ray diffraction analyses are usually less sensitive to vertical parameters than LEED ones. However, there is an interesting feature concerning the medium-energy ion scattering measurements of the same research group [15]. The authors state that their data are well described using a tilted-chain model, but equally well interpreted in terms of non-tilted chains when the vibrational amplitudes of the surface atoms are enlarged by a factor of two compared to the bulk value [15]. Interestingly, we find that the vibrational amplitudes resulting from our fit are indeed enlarged, with root mean square displacements of 0.14 and 0.12 Å for the first and second layer, respectively (compared to a bulk value of 0.06 Å).

Before discussing the other parameters determined and displayed in the table, we address—in the light of the missing tilt—the issue of chain dimerization, i.e. the question of whether the bonds within the chain are of equal length or whether shorter and longer lengths alternate. As mentioned in the above sections, we allowed also for lateral relaxations for the atoms in the two outermost bilayers but cannot expect the same accuracy as for the vertical parameters (indeed, the comparison is 0.03 versus 0.10 Å as given above). The analysis yields values of l_1 and l_2 (see figure 1) which produce a rather small dimerization, $d = |l_1 - l_2| / (l_1 + l_2) = 0.7\%$ with, however, an error margin of 6%, so the upper limit is $d \approx 7\%$. Of course, in principle

Table 1. Comparison of the results of the present LEED analysis with those of first-principles calculations [23]. The parameters displayed are defined in figure 2; the quantities d_{bi} and d_{ik} refer to the centre-of-mass planes of the subplanes involved. The bulk values for C(111) are $d_0 = l_0 = 1.544 \text{ \AA}$, $d_b^0 = 0.515 \text{ \AA}$.

Structural parameter	LEED (this work) (\AA)	DFT (\AA) [23]
$d_{12} (\Delta d_{12}/d_0)$	1.55(+0.4%)	—
$d_{23} (\Delta d_{23}/d_0)$	1.55(+0.4%)	—
$d_{34} (\Delta d_{34}/d_0)$	1.52(−1.5%)	—
d_{b1}	0.68	—
$d_{b2} (\Delta d_{b2}/d_b^0)$	0.51(−1%)	—
$d_{b3} (\Delta d_{b3}/d_b^0)$	0.50(−3%)	—
$d_{b4} (\Delta d_{b4}/d_b^0)$	0.51(−1%)	—
b_{11}	0.01	<0.01
b_{12}	0.01	0.01
b_{21}	0.02	0.03
b_{22}	0.18	0.17
b_{31}	0.08	0.06
b_{32}	0.01	0.02
b_{41}	0.01	Fixed at 0
b_{42}	0.04	Fixed at 0
$l_{12} (\Delta l_{12}/l_0)$	1.62(+4.9%)	1.60(+3.6%)
$l'_{12} (\Delta l'_{12}/l_0)$	1.64(+6.2%)	1.63(+5.6%)
$l_{23} (\Delta l_{23}/l_0)$	1.61(+4.3%)	1.60(+3.6%)
$l'_{23} (\Delta l'_{23}/l_0)$	1.49(−3.5%)	1.49(−3.5%)

the lateral sensitivity of LEED could be increased by using off-normal-incidence intensity data as, e.g., applied in the determination of the in-plane reconstruction of W(100) [31]. Yet, the procedure requires the angles of incidence as additional fit parameters and the averaging of beam intensities degenerate at normal incidence is no longer possible, leading to data of lower quality.

Table 1 also reveals how the surface reconstruction continues into deeper layers towards the bulk, an issue of particular importance for materials with—as in the present case of diamond—strongly localized bonds. Apparently, the lower sublayer of the second bilayer is substantially buckled, with atoms constituting the lower corner of the sevenfold ring shifted outward and those of the fivefold ring shifted inward, with the difference amounting to as much as 0.18 \AA . These shifts continue—though less pronounced—to the neighbouring atoms of the upper sublayer of the next bilayer in such a way that the corresponding bond length l_{23} (l'_{23}) is expanded (contracted). Even in the fourth bilayer there is considerable buckling, though we should note that this is no longer outside our error limits, as they increase with depth because of electron attenuation.

4. Discussion and conclusions

The above LEED structure analysis of C(111) (2×1) shows—in contradiction to earlier experimental work [14]—that the π -bonded chains forming the (2×1) surface reconstruction are *not* (or are only negligibly) tilted. A plausible reason for diamond having untilted chains, whilst chains in Si and Ge exhibit a strong tilt, might be the more localized nature of carbon bonds, leading to a weaker interaction of the bands and therefore a smaller energy gain when

breaking symmetry. So, tilted chains cannot be responsible for the band gap detected by angle-resolved photoelectron spectroscopy [10, 11] and electron energy-loss spectroscopy [12, 13]. (Theoretical work concludes that buckling would not even lead to a band gap [32].) Instead, in the light of our present understanding, some dimerization must be responsible. Though the respective value determined in the present work is rather small, $d = 0.7\%$, our error limits allow values as large as $d \approx 7\%$, i.e. larger than all values realistically discussed.

As also displayed in table 1, our result of untilted chains *and* the result for the structure of the bilayers below compare extremely well with the structure obtained by *ab initio* calculations which also consider the relaxations of deeper bilayers [23]. In the latter work, density functional theory in the local-density approximation (LDA) was used, but when the generalized gradient approximation (GGA) is applied—which is more appropriate for a strongly localized system like diamond—the results do not change very much [24]. In agreement with our result for the chain structure, there is neither a substantial tilt nor dimerization. We note, however, that in an earlier *ab initio* molecular dynamics study [18] a dimerization of $d = 1.4\%$ was retrieved, i.e. not deviating too much from our value, and that this—by consideration of many-electron effects—can lead to a band gap as large as 1.7 eV [32] which is in the range of the experimentally determined value. We also mention that metastable states with a strong dimerization of the lower-lying chain have been found in recent Monte Carlo simulations [33].

Concerning the subsurface structure, it is evident that the surface reconstruction protrudes into the surface down to the fourth bilayer. A substantial buckling of the sublayers is induced, i.e. all bilayers included in our structural analysis exhibit the (2×1) symmetry of the very surface. The theoretical predictions and the present experimental results agree within about one per cent also for the subsurface structure. Judging by this excellent comparison between theory and experiment, the problem of the geometric structure of C(111) (2×1) appears to be resolved, though the precise origin of the surface band gap remains less clear.

References

- [1] Derry T E, Smit L and van der Veen J F 1986 *Surf. Sci.* **167** 502
- [2] Pandey K C 1982 *Phys. Rev. B* **25** 4338
- [3] Pandey K C 1981 *Phys. Rev. Lett.* **47** 1913
- [4] Himpsel F J, Marcus P M, Tromp R, Batra I P, Cook M R, Jona F and Liu H 1984 *Phys. Rev. B* **30** 2257
- [5] Smit L, Tromp R M and van der Veen J F 1984 *Surf. Sci.* **163** 315
- [6] Sahama H, Kawazu A and Ueda K 1986 *Phys. Rev. B* **34** 1367
- [7] Bechstedt F, Stekolnikov A A, Furthmüller J and Käckel P 2001 *Phys. Rev. Lett.* **87** 016103
- [8] Hirayama H, Sugihara N and Takayanagi K 2000 *Phys. Rev. B* **62** 6900
- [9] Sowa E C, Kubiak G D, Stulen R H and Van Hove M A 1988 *J. Vac. Sci. Technol. A* **6** 832
- [10] Himpsel F J, Eastman D E, Heimann P and van der Veen J F 1981 *Phys. Rev. B* **24** 7270
- [11] Graupner R, Hollering M, Ziegler A, Ristein J, Ley L and Stampfl A 1997 *Phys. Rev. B* **55** 10 841
- [12] Pepper S V 1982 *Surf. Sci.* **123** 47
- [13] Namba H, Masuda M and Kuroda H 1988 *Surf. Sci.* **33/34** 187
- [14] Huisman W J, Lohmeier M, van der Vegt H A, Peters J F, de Vries S A, Vlieg E, Etgens V H, Derry T E and van der Veen J F 1998 *Surf. Sci.* **396** 241
- [15] Huisman W J, Peters J F and van der Veen J F 1998 *Surf. Sci.* **396** 253
- [16] Chin R P, Huang J Y, Shen Y R, Chuang T J and Seki H 1995 *Phys. Rev. B* **52** 5985
- [17] Bechstedt F and Reichardt D 1988 *Surf. Sci.* **202** 58
- [18] Iarlori A S, Galli G, Gygi F, Parrinello M and Tosatti E 1992 *Phys. Rev. Lett.* **69** 2947
- [19] Frauenheim Th, Stephan U, Blandeck P, Porezag D, Busmann H-G, Zimmermann-Edling W and Lauer S 1993 *Phys. Rev. B* **48** 18 189
- [20] Saito M, Oshiyama A and Miyamoto Y 1998 *Phys. Rev.* **57** R9412
- [21] Vanderbilt D and Louie S G 1983 *J. Vac. Sci. Technol. B* **1** 723
- [22] Schmidt W G, Scholze A and Bechstedt F 1996 *Surf. Sci.* **351** 183
- [23] Kern G, Hafner J and Kresse G 1996 *Surf. Sci.* **366** 445

- [24] Saito M, Oshiyama A and Miyamoto Y 1999 *Surf. Sci.* **427** 53
- [25] Heinz K 1995 *Rep. Prog. Phys.* **58** 637
- [26] Watson P R, Van Hove M A and Hermann K 2001 *NIST Surface Structure Database Version 4.0* National Institute of Standards and Technology, Gaithersburg, MD
- [27] Pendry J B 1980 *J. Phys. C: Solid State Phys.* **13** 937
- [28] Blum V and Heinz K 2001 *Comput. Phys. Commun.* **134** 392
- [29] Pendry J B 1974 *Low-Energy Electron Diffraction* (London: Academic)
- [30] Kottcke M and Heinz K 1996 *Surf. Sci.* **376** 352
- [31] Schmidt G, Zagel H, Landskron H, Heinz K, Müller K and Pendry J B 1992 *Surf. Sci.* **271** 416
- [32] Kress C, Fiedler M and Bechstedt F 1994 *Europhys. Lett.* **28** 433
- [33] Petukhov A V, Passerone D, Ercolessi F, Tosatti E and Fasolino A 2000 *Phys. Rev. B* **61** R10 590